

# Study of GEM Characteristics for Application in a Micro-TPC

B. Yu, V. Radeka, G. C. Smith, C. L. Woody, and N. N. Smirnov

**Abstract**—The Gas Electron Multiplier (GEM) may provide a convenient method for obtaining significant electron multiplication over large areas. An important potential application of the GEM is for readout of microTPCs. We are conducting a study of a multi-GEM structure with particular emphasis on its performance with respect to gain uniformity/stability, ion feedback and position readout. In particular, we present the first experimental results of interpolating anode pad readout. Initial results provide encouragement that the GEM application in microTPCs may be realized.

## I. INTRODUCTION

The Gas Electron Multiplier (GEM), developed by the Gas Detector Group (GDD) at CERN [1], offers great potential as a high resolution tracking detector for a variety of applications. One such application is tracking particles in the high multiplicity environment of relativistic heavy ion collisions at RHIC, where one needs not only excellent spatial resolution, but also large solid angle coverage and high rate capabilities. A possible approach to meet these needs would be to incorporate the features of the GEM detector into a small, fast MicroTPC which would provide tracking coverage starting at a relatively close distance ( $\sim 20$  cm) to the collision vertex, and would have a sufficiently fast drift time to be able to operate at the highest rates envisioned for RHIC[2]. However, these requirements place stringent demands on the performance of the GEM detector, and a study has therefore been made to evaluate the suitability of the GEM as an amplification stage for such a MicroTPC.

The measurements are focused on the gas gain uniformity, stability, ion feedback and interpolating readout of the detector. A two stage GEM was provided by the GDD group at CERN. It consisted of GEM foils which were  $50 \mu\text{m}$  thick, with a hole pitch of  $140 \mu\text{m}$  and a hole diameter of  $80 \mu\text{m}$  copper and  $60 \mu\text{m}$  kapton. The active area was  $10 \times 10 \text{cm}^2$ . The foils were arranged with a 3 mm drift depth, and 2 mm transfer and induction depths. All results shown in this report have been obtained with a gas mixture of  $\text{Ar}+20\%\text{CO}_2$ .

## II. GAS GAIN UNIFORMITY AND STABILITY

Manuscript received Dec. 2, 2003. This work was supported by the U.S. Department of Energy under Contract No. DE-AC02-98CH10886

B. Yu (yu@bnl.gov), V. Radeka (radeka@bnl.gov), G.C. Smith (gsmith@bnl.gov) and C.L. Woody are with Brookhaven National Laboratory, Upton, NY 11973.

N. N. Smirnov (smirnov@star.physics.yale.edu) is with Yale University, New Haven, CT 06520

TPCs designed to use  $dE/dx$  information for particle identification require good energy resolution. Under a collimated  $5.4\text{keV}$  x-ray beam, the energy resolution of the double GEM structure was measured to be 17% FWHM with  $V_{\text{GEM}}=400\text{V}$  (gas gain  $\sim 6000$ ). It maintained similar energy resolution over a gas gain range of 500 through  $10^4$ .

The gas gain uniformity of the double GEM detector was measured using a collimated x-ray beam of about  $1\text{mm}^2$  in size. The beam was moved in 1mm steps to form a raster scan over a  $9\text{cm} \times 9\text{cm}$  area of the detector. At each step, over 10,000 events were histogrammed, and a Gaussian curve was fitted to the photopeak. Gas gain variation due to barometric pressure was corrected using a reference wire counter downstream of the gas flow. The gain map is shown in fig. 1. The overall variation in the gas gain is about  $\pm 20\%$ .

The dependence of gas gain on the x-ray flux has also been studied. The double GEM was irradiated under a  $1\text{mm}^2$  pencil beam of x-rays. The x-ray flux was changed from time to time and the pulse height of the photo peak was recorded. The results, shown in fig. 2, clearly show the GEM gas gain is influenced by the photon flux. This is inconsistent with published results from the CERN group [3]. A shift is observed in the gas gain that depends on the previous history

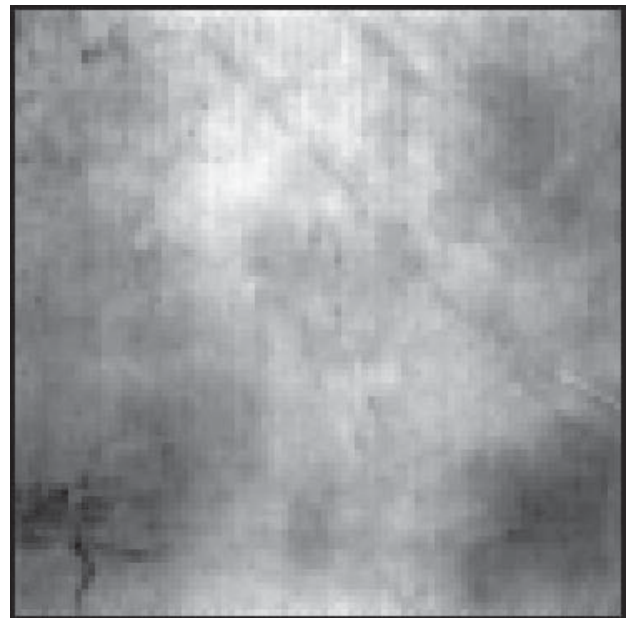


Fig 1. The gas gain map of the double GEM detector. A  $1\text{mm}^2$  x-ray beam was used to scan the  $9 \times 9 \text{cm}^2$  area at a  $1\text{mm} \times 1\text{mm}$  grid. The relative gas gain varies from 91 (black) to 146 (white) on an arbitrary scale.

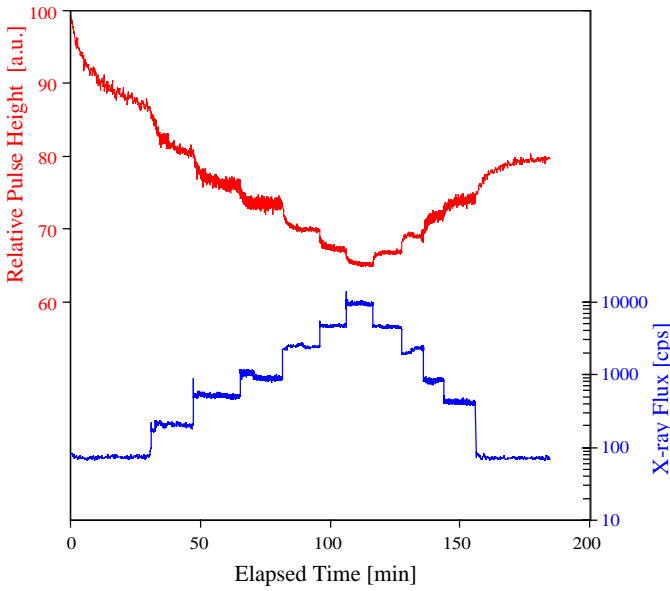


Fig 2. Gas gain variation of the double GEM under different x-ray flux. The relative pulse height curve, shown in red is the position of the photo peak from 1000 events (rate under 1kcps) or 10000 events (rate over 1kcps). 1mm<sup>2</sup> 5.4keV x-ray flux, shown in blue, varies from 80cps to 10kcps. The effective gas gain is about 600.)

of the x-ray flux: If the GEM has been exposed to a low flux of x-rays, a sudden increase of flux will result in a downward drift of the pulse height until it levels off. Conversely, if the GEM has been exposed to a high flux, a sudden reduction in flux will lead to an upward drift of the pulse height. This behavior can be clearly seen in fig.2. This behavior has been observed on two independent double GEM detectors. However, the magnitude of gain reduction under a fixed flux varies with location on the detector. At these photon rates ( $\sim$ kHz/mm<sup>2</sup>), it is highly unlikely that the gain reduction is due to space charge buildup. The very long time constants in the gain shift seem to indicate another kind of charging effect, different from the initial charging phenomenon reported in ref. 3.

### III. POSITIVE ION FEEDBACK

Space charge distortion in the drift volume is a major factor limiting the performance of a TPC operating under high flux.. While the space charge buildup from the primary ionization is inevitable, those positive ions coming from the amplification region should be minimized. The ion feedback fraction is used in this work to quantify the unwanted positive ions relative to the signal forming electrons. It is defined as the ratio of the currents flowing into the cathode window and the anode plane:  $f_i = I_w/I_a$ . In a chamber with gas amplification,  $G$ , a practical lower limit for the ion feedback is  $1/G$ . At this level, the contribution to the space charge from amplification region is similar to that from the primary ionization.

Traditional TPCs with MWPC as the amplification medium routinely employ active gating grids to curtail the ion buildup in the drift volume. However, in a microTPC, with

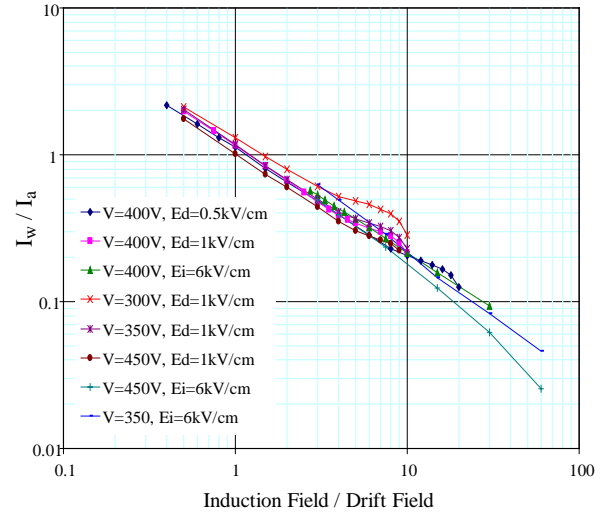


Fig. 3 Ion feedback as a function of the ratio of the induction field and the drift field. Ar + 20% CO<sub>2</sub>, 8mm drift gap, 2mm induction gap.

a total drift time of only a few microseconds, the triggering latency and settling time required for gating will significantly reduce the usable drift length of the TPC. With the introduction of GEM, it has been hoped that the highly opaque geometry of the GEM may eliminate the need for the gating grid.

#### A. Single GEM

A large collection of ion feedback measurements with a single gem is plotted as functions of the field ratios below (induction field,  $E_i$ ) and above (drift field,  $E_d$ ) the GEM foil in fig. 3. The operating parameters in these measurements vary over a large range. However, the data points from these measurements congregate along a narrow band. The general form of the data points can be described by:

$$I_w/I_a = (E_d/E_i)^{0.7}$$

Another minor factor that affects the ion feedback rate is the GEM gain. A higher gas gain reduces the ion feedback rate slightly, a likely result of the increased avalanche region under higher gain.

#### B. Double GEM

There have been a large number of works on current measurements with double GEMs[4]. Our measurements show similar results: In general, the ion feedback

1. is a linear function of the drift field, until the value of the drift field approaches that of the transfer field;
2. has strong dependence on the induction field;
3. has moderate dependence on the gas gain;
4. has a weak dependence on the transfer field.

In addition, the measurements in this work indicate a weak dependence of ion feedback on the distribution of gain between the two GEM stages, for a constant total gain. A larger gain in the second GEM gives a slightly lower ion feedback fraction and visa versa.

At 1kV/cm drift field, the best ion feedback fraction is

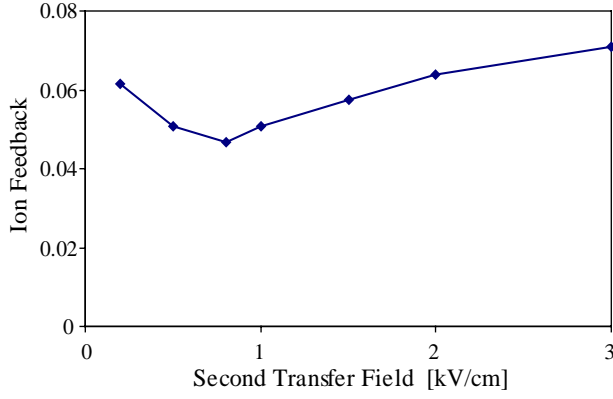


Fig. 4 Ion feedback as a function of the second transfer field.  $E_d = 1\text{ kV/cm}$ ,  $E_{t1} = 4\text{ kV/cm}$ ,  $E_i = 4\text{ kV/cm}$ ,  $V_{\text{GEM}} = 400\text{ V}$ .

about 15%.

### C. Triple GEM

The additional GEM stage does not reduce the ion feedback fraction if the fields at each gap are progressively increasing for efficient electron transfer, ie:  $E_d < E_{t1} < E_{t2} < E_i$ . However, if the first transfer field is set lower than the drift field ( $E_d > E_{t1} < E_{t2} < E_i$ ), or the second transfer field is set lower than the first transfer field, ( $E_d < E_{t1} > E_{t2} < E_i$ ), the ion feedback fraction can be further reduced. Reducing the value of the first transfer field below that of the drift field should be avoided, since it may affect the collection of the primary electrons. Fig. 4 shows the results with the reduced second transfer field.

As an approximation, a GEM foil can be treated like a plane of mesh, for the purpose of the transport of ions. The strong electric field inside the GEM holes makes the GEM foil much more transparent than the optical transparency of the foil. The fractional ion transfer,  $f$ , through each GEM foil is largely determined by the field ratio of the exit side to the entrance side the foil:

$$f \sim E_{\text{exit}} / E_{\text{entrance}}, \quad \text{if } E_{\text{exit}} < E_{\text{entrance}}$$

$$f \sim 1, \quad \text{if } E_{\text{exit}} > E_{\text{entrance}}$$

The reduction in ion feedback fraction in this case (fig. 4) is largely due to the two favorable field ratios  $E_d/E_{t1}$  and  $E_{t2}/E_i$ . However, the electron transfer through the second GEM also suffers a large reduction, resulting in a much lower effective gain.

## IV. INTERPOLATING PAD READOUT

In order to develop optimized pad readout for position encoding in a TPC, the spread of the GEM avalanche electrons at the anode plane needs to be measured. A collimated  $100\mu\text{m}$  wide  $5.4\text{ keV}$  x-ray beam was used to scan in  $100\mu\text{m}$  steps across a set of 4 adjacent anode strips at  $400\mu\text{m}$  pitch. The most probable pulse height from each channel was recorded for each x-ray beam position and is shown in fig.5. The FWHM of the spread is about  $0.5\text{ mm}$ . This result indi-

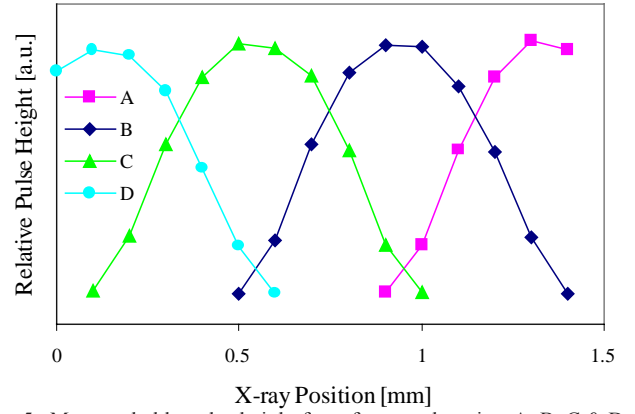


Fig. 5. Most probable pulse height from four anode strips, A, B, C & D, on a  $400\mu\text{m}$  pitch as a function of the x-ray beam position.

cates that in order to achieve an efficient position interpolation with good linearity, the basic feature size of the pads should be slightly under  $0.5\text{ mm}$ . [5].

Another test chamber was constructed with several different types of interpolating pad arrays on the anode plane. Similar patterns have been tested and used as interpolating cathode readout in MWPCs [6]. The size of the pads are  $2\text{ mm} \times 10\text{ mm}$ , a baseline choice for the TPC. The interpolation is along the  $2\text{ mm}$  direction. The linearity of these anode pad arrays was determined by measuring their uniform irradiation responses (UIRs), which are histograms of reconstructed positions from a large number of radiation events uniformly distributed over the detector. A perfect detector should exhibit a flat response.

### 1. Zigzags

Zigzag, or chevron shaped, pads have been used in many position sensitive MWPC applications [7,8]. They are better suited for MWPCs because the induced charge distribution is centered along an anode wire, which has a fixed relative position with respect to the zigzag pattern. However, in the case of GEM, the final electron jet can arrive at arbitrary positions with respect to the zigzag pattern.

Two zigzag pad designs were tested with a double GEM structure. One zigzag pattern (coarse) has a period of  $1\text{ mm}$  (fig. 6a), while the other (fine) has a period of  $0.5\text{ mm}$  (fig. 7a).

The UIR from the coarse zigzag pattern was surprisingly good (fig 6b), but additional measurement with a collimated x-ray beam revealed some unfavorable characteristics. The x-ray beam ( $0.1\text{ mm} \times 3\text{ mm}$ ) was used to scan the zigzag pattern at  $0.1\text{ mm}$  steps. The position response of the zigzag pattern is recorded for each of the x-ray beam positions. The results are shown in fig. 6c. Not only the peaks are broad, but at certain locations in the detector, the peaks are split into two. The double peak can be easily explained by analyzing three x-ray events centered on the each of the three circles in fig. 6a. The size of the circles roughly represents the FWHM of the charge spread on the pad plane. The top

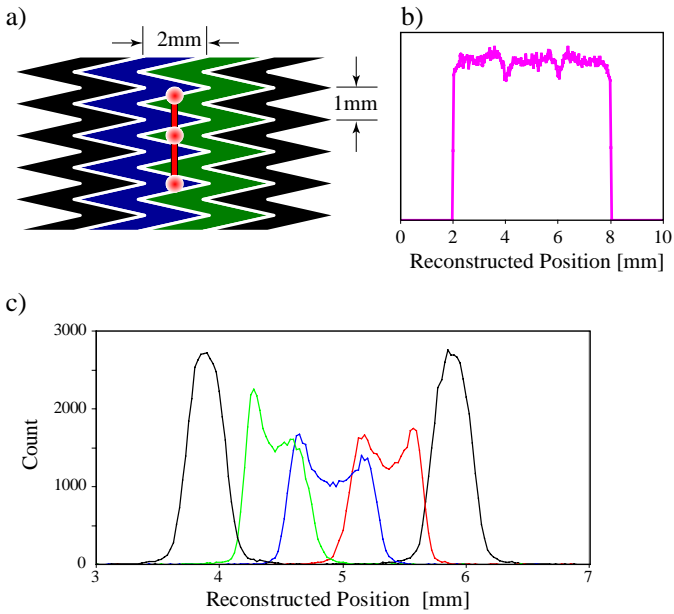


Fig. 6 a) Coarse zigzag pattern, b) its uniform irradiation response, and c) position responses of a line beam.

event should give rise to equal amount the charge on two pads, results in a reconstructed position midway between the two readout node. The middle event deposits most of its charge on the pad to the right, results in a reconstructed position displaced to the right. Similarly, the bottom event is displaced to the left. Given a large number of events distributed along the vertical line of these circles, the reconstructed position histogram will have a double peak.

Similar measurements were performed on the fine zigzag pattern with good results (fig. 7a). Even though the UIR exhibits large peaks, the overall rms error of the detector is better than  $100\mu\text{m}$ . This figure includes the contribution of  $\sim 100\mu\text{m}$  FWHM of the x-ray photo electron range,  $100\mu\text{m}$  beam size, and the systematic errors of the zigzag pattern. This figure only represents the detector's x-ray point response. Position resolution for a track segment is expected to be better.

## 2. Intermediate Strip Patterns

Several intermediate strip patterns are tested (fig 7b-d)[8]. These designs use one or two "intermediate" strip(s) that are "floating" between two adjacent readout strips. The charge induced on these floating strips are capacitively coupled to their neighboring readout strips. In practice, the "floating" strips are held to the right bias through high value resistors. A key point in design these patterns is that the inter-strip capacitance needs to be much higher than the strip capacitance to ground. The zigzag pattern is ideal for this purpose. The zigzag periods of all the patterns are  $0.5\text{mm}$ , fine enough to give good interpolation. There is no sign of double peaks in the collimated beam tests, and the absolute systematic errors are less than  $\pm 80\mu\text{m}$ .

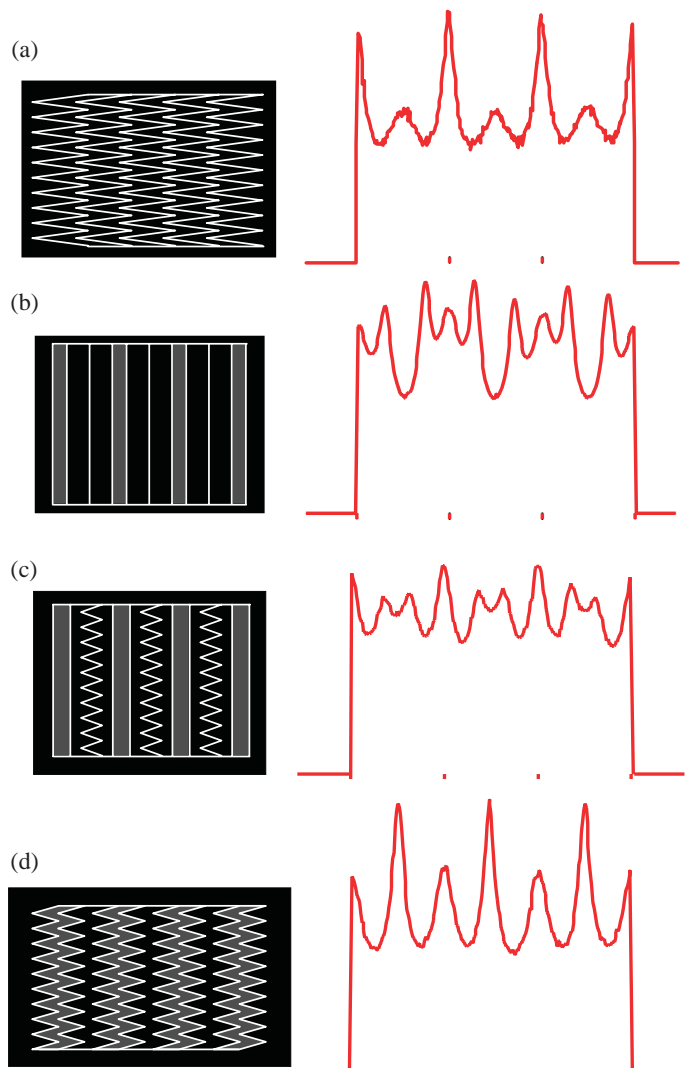


Fig. 7. Several interpolating pad pattern and their uniform irradiation responses measured in the double GEM chamber. (b) and (c) have two intermediate strips, and (d) has a single intermediate strip. The readout strips in (b,c,d) are lightly shaded.

## V. DISCUSSION

The gas gain uniformity in our test chamber is somewhat larger than anticipated. Further study with other GEM foils is needed to identify the cause of the variation and its long term stability. The non-uniformity can be corrected in a TPC through calibration if it is stable over time.

The gain dependence on flux is apparent at relatively low photon flux. In the RHIC operating environment this TPC is envisioned, the particle rate is well under the 100 cps per  $\text{mm}^2$  equivalent x-ray flux shown in fig. 2. However, for other high rate tracking and x-ray imaging applications, this would pose an interesting calibration problem.

Since the ion feedback fraction can be dramatically reduced by lowering the drift field, it may lead to the conclusion that with a low drift field, the ion space charge effect can be alleviated. However, there is a simple argument against it:

Assuming the ion feedback rate  $f_i$  has a linear dependence on the drift field  $E_d$ :  $f_i = a E_d$ , and the total primary ionization current entering the amplification region remains constant  $I_0$ . The total current of positive ion drifting into the TPC volume at any given time is:  $I_i = I_0 G_{\text{eff}} f_i$ . The net charge density in the TPC drift volume is:  $\sigma_i = I_i / v_i$ , where  $v_i$  is the drift velocity of the ions:  $v_i = \mu E_d$ . Therefore:

$$\sigma_i = I_0 G_{\text{eff}} a E_d / (\mu E_d) = a I_0 G_{\text{eff}} / \mu.$$

Thus the positive ion charge density in the drift volume is independent of  $E_d$ . This fixed quantity of net charge in the drift volume creates a distortion field  $E'(\sigma_i)$ , which is independent of  $E_d$ . However, the deflection to the field lines in the drift region is determined by the relative distortion:  $E'(\sigma_i) / E_d$ , therefore the distortion is less significant in a stronger drift field.

It has been demonstrated that simple geometrical and capacitive charge division schemes such as zigzag strips and intermediate strips can be used with GEM to achieve moderate interpolating ratios ( $\sim 20$ ). Resistive charge division [9] will perform well for one dimensional/projective readout. Two dimensional pad readout with resistive charge division [10] maybe difficult to realize due to the precision resistive connection required between rows of pads. In general, compared to the single zigzag pattern, the intermediate strip patterns have lower capacitive load to the preamplifiers; there is more room for plated through hole connections. However, they do require additional resistive connections between the "floating" strips and their neighboring readout strips. A small percentage of charge induced on the floating strips are lost to the ground, potentially broadening the energy resolution of the detector.

## VI. ACKNOWLEDGMENTS

The authors would like to thank Dr. F. Sauli for providing the test chamber and additional GEM foils.

## VII. REFERENCES

- [1] F. Sauli, "GEM: A New Concept for Electron Amplification in Gas Detectors". Nucl. Instrum. & Meth. A386 (1997) 531.
- [2] N. Smirnov et al., "A Fast, Compact Time Projection Chamber and Cherenkov Detector for Tracking and Electron Identification in Heavy Ion Collisions," presented at this conference.
- [3] R. Bouclier et al., "New observations with the gas electron multiplier (GEM)," Nucl. Instrum and Meth A 396 (1997) 50-66.
- [4] S. Bachmann et al., "Charge amplification and transfer processes in the gas electron multiplier," Nucl. Instrum. and Meth. A438 (1999) 376-408.
- [5] E. Gatti et al., "Optimum geometry for strip cathodes or grids in MWPC for avalanche localization along the anode wires," Nucl. Instrum. and Meth. 163 (1979) 83-92.
- [6] G.C. Smith and B. Yu, "The Linearity Performance of a Two-Dimensional, X-ray Proportional Chamber with 0.58 mm Anode Wire Spacing," IEEE Trans. Nucl. Science, Vol 42, 1995 pp. 541-547.
- [7] T. Miki, R. Itoh and T. Kamae, "Zigzag-shaped pads for cathode readout of a time projection chamber," Nucl. Instrum. and Meth. A236 (1985), 64-68.
- [8] E. Mathieson and G.C. Smith, "Reduction in non-linearity in position-sensitive MWPCs," IEEE Trans. Nucl. Sci. NS-36 (1989), 305-310.
- [9] J. L. Alberi and V. Radeka, "Position Sensing by Charge Division," IEEE Trans. Nucl. Sci NS-23 (1976), pp.251-258.
- [10] R. Debbe et al., "MWPC with Highly Segmented Cathode Pad Readout," Nucl. Instrum. Methods, A283 (1989) pp.772-777.